RESEARCH ON RELATIONSHIP BETWEEN ELECTRICAL RESISTANCE TOMOGRAPHY AND THE MULTIPLE-SCALE SIZE AND DEPTH OF ROCK FRACTURE

Fan Jing, Nanjing University, Nanjing, P. R. China
Li Xiao-Zhao, Nanjing University, Nanjing, P. R. China
Alessandro Tarantino, University of Strathclyde, Glasgow, UK
Huang Zhen，Nanjing University, Nanjing, P. R. China
Bruna De Carvalho Faria Lima Lopes, University of Strathclyde, Glasgow, UK

ABSTRACT

Multiple sets of cracks exist in the fault fracture zone, damage zone and even intact rock mass, resulting in poor conductivity and high permeability of the hard rock fissure seepage channels. Therefore, there is high likelihood for groundwater migration channels in the future, thus underground engineering is facing huge challenges. To more accurately grasp the characteristics of the permeability of rock mass and fracture, it is extremely important to get hold of the phenomena of internal structure model, genetic mechanism and dynamics principle in the multiple-scale size and depth of rock fracture. Accurate analysis of the multiple-scale of rock mass fracture, mastering the principles and patterns of the solute and flow medium migration rule in pore and fracture can provide scientific basis for underground construction engineering.

In this paper, the multiple-scale size and depth of rock fracture were investigated using ERT in the physical model tests, forward and inversion software simulation and site detection. The results show that small scale crack has a good physical effect with ERT. Combined with the ERT measurement results of water conducted zone in the typical research area, rock fracture with many lines are arranged in parallel and the vertical direction of the fault, which are in conformity with the physical model tests. The results provide great progress in the precise exploration of geophysical detecting on the multiple-scale size and depth of rock fracture.

Introduction

Electrical Resistance Tomography (ERT) has the characteristics of undisturbed, non-radiation, visualization and on-line measurement. ERT has application prospects in two-phase flow measurement (Buselli G, Lu K, 2001. Maineult A, Barnabé Y, et al, 2004. Nimmer RE, Osiensky JL, 2002. Revil A, Naudet V, et al, 2003.). The signal generator module of the ERT data acquisition system is usually composed of analog and Direct Digital Frequency synthesizer (DDS) type (Rizzo E, Suski B, et al, 2004. Atekwana EA, Werkema DD, et al, 2004. Berger W, Börner F, et al, 2001. Berthold S, Bentley LR, et al, 2004. Boerner FD, 2001.). Among them, DDS has a higher frequency resolution, which can achieve fast frequency switching. And the frequency, phase and amplitude of numerical control modulation can be easily realized when the frequency change can be maintained in a continuous phase (Comas X, Slater L, 2004. Fechner T, Boerner FD, et al, 2004. Dresden. Grissemann C, Rammlmair D, et al, 2000. Kemna A, 2000. Kemna A, Binley A, et al, 2004. Klitsch N, 2003.). The DDS chip AD7008 and peripheral circuit formed the signal generation module of the ERT data acquisition system, producing frequency, amplitude, and phase tunable sine wave.

Supported by the Geotechnical and geological Responses to climate change: Exchanging Approaches and Technologies on a world-wide scale International Research Staff Exchange Scheme (IRSES).

It claims that this paper is for the special session of "Geophysics for Urban Underground Space Development".

Fan Jing (1989–), male, School of Earth Sciences and Engineering, Nanjing University, Nanjing, Jiangsu Province, 210046, P. R. China. Studying on Rock fracture system and characteristic identification. E-mail：fanjing200808@163.com.

Optimizing the best to have the test designed to detect resistance tomography (ERT) system technology to detect rock fracture development regularities, grouting plugging technology reshape rock lead water performance and geotechnical engineering geological research more in-depth study (Lesmes DP, Frye KM, 2001. Liu S, Yeh T-CJ, 2004. Niederleithinger E, Grissemann C, et al, 2000. Slater LD, Lesmes DP, 2002a.).

Understanding the advanced scientific research ideas, mastering the technical inspection of the ERT seal rock fracture rules, grouting technique to improve the performance of water and rock mass research means, to understand foreign related technology and the present situation of the application (Slater LD, Lesmes DL, 2002b. Titov K, Komarov V, et al, 2002. Titov K, Kemna A, et al, 2004. Ulrich C, Slater LD, 2004.).

ERT technique is in the response characteristics of the fracture of rock mass under different scales, hard rock fracture well. Research on relationship between refined geophysical interpretation methods and serous migration of hard rock fracture, including mechanism and the permeability coefficient of correlation, it can provide petrophysical parameters for underground construction and rock engineering.

The principle of theory

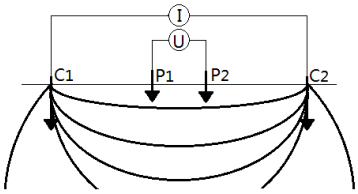

Fig.1 Principle of geo-electrical measurement

Principle of geo-electrical measurement is injecting direct (DC) current into the measured soil using two current electrodes C1, C2 and measuring induced potential on two potential electrodes P1, P2 (Fig.1). Apparent resistivity $\rho_a[\Omega m]$ is calculated from electrode positions, current and potential by the equation (1)：

$$\rho_a = k\frac{\Delta V}{I} \qquad (1)$$

Where $\Delta V[mV]$ is measured voltage, $I[mA]$ is current and K is geometrical factor depending on the individual distance (2) between the electrodes (Fig.2).

$$k = \frac{2\pi}{\frac{1}{r_{C1\,P1}} - \frac{1}{r_{C2\,P1}} + \frac{1}{r_{C2\,P2}} - \frac{1}{r_{C}}} \qquad (2)$$

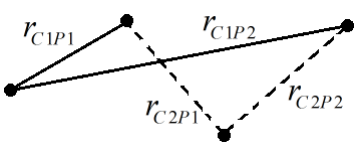

Fig.2 Position of current electrodes

The geometric factor for subsurface electrodes is different from that used for surface electrodes. Reflected image of the current electrode C' is added to the equation(3) (Fig.3)：

$$K = \frac{4\pi}{\frac{1}{r_{C1P1}} + \frac{1}{r'_{C1'P1}} + \ldots} \qquad (3)$$

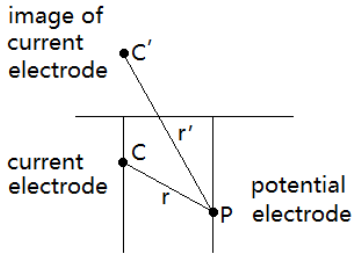

Fig.3 Reflected image of the current electrode

Three electrode arrays (pole-dipole) and two electrode arrays (pole-pole) are also used for geo-electrical measurement. Remaining electrodes, called infinite or remote electrodes, are distant enough from the electrode arrays thus their influence can be ignored. With sufficient number of measured points, we can do 1D, 2D, 3D, and also 4D (time monitoring) data processing for imaging of studied structures. Several positive and negative current pulses are measured for elimination of noise and drift (e.g. influence of artificial and telluric currents, electrode polarization). The standard deviation of the measurement δ (St-dev) is calculated as follows (4):

$$\delta = \frac{1}{\overline{R}} \sqrt{\frac{\sum (\overline{R} - R)^2}{N - 1}} 100\% \qquad (4)$$

Where R is measured resistance, $\overline{R}$ is **arithmetic mean value** and N is the number of repeated measurements.

Also, the potential **decay curve** after switching current off can be measured. The residual potential (which disappears in tenths of milliseconds or units of seconds) is measured in several time windows. Those values are used for calculating of induced polarization (IP) as a ratio of the measured potential in a certain IP window and the potential before switching current off. See equation (5).

$$ip[\%] = \frac{U_{ip}}{U} 100 \qquad (5)$$

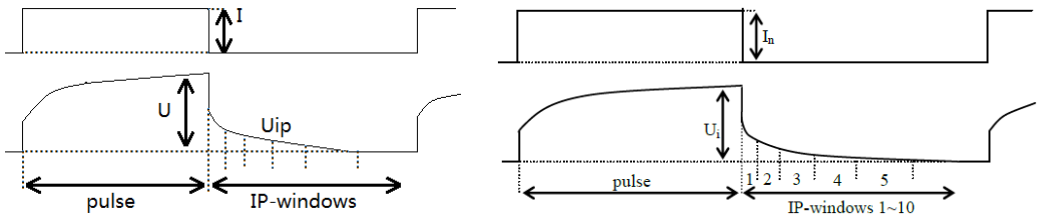

Fig.4 Measurement of induced polarization IP

ARES II with its 10-channel receiver allows simultaneous measurement of several potential responses and thus makes the measurement faster. 10 channels (from R0 to R9) are measured between potential electrode couples P1-P2 to P10-p11 (Fig.4).

Methods of geo-electrical measurement

2D-multi-electrode measurement is an up-to-date method which uses fully automatic measurement of sections of apparent resistivity of induced polarization. It allows doing a very

detailed investigation of both vertical and horizontal structures and imaging of objects with different resistivity. There are various measuring arrays convenient for optimum sensitivity for different kinds of structures (vertical/horizontal structures, cavities). This method is used e.g. for determination of geological sections, imaging of fissures, water leakages, slope deformations and landslides (Weihnacht B, Boerner F, 2005. Ahl A, 2003. Bosch FP, Gurk M, 2000. Auken E, Jørgensen F, et al, 2003.).

For the measurement a multi-electrode cable is needed, whose number of outlets is grounded on electrodes at regular intervals on a straight line. The device automatically chooses the electrodes to be used for measurement by chosen prescription. It is possible to obtain many hundreds of measured points in an hour. Several times more points can be obtained using 10-channel ARES II. The result of the measurement is 2D section, which should be interpreted in proper software (e.g. Res2DInv). It is also possible to assemble several 2D measurement for interpreting in one 3D model (so called pseudo 3D measurement).Measuring of 2D is done by prescription, which is uploaded into device memory. Multi-electrode cable (active or passive version). One multi-electrode section contains 4-12 outlets (depending on spacing between electrodes). Individual sections can be connected up to 60000outlets (resp. 200outlets of single-channel multi-electrode cable). The total length of multi-electrode cable determines reachable measurement depth. T-piece allows connecting the device between any two active cable sections. Electrodes for all multi-electrode cable outlets. O-rings for attaching of the outlets to the electrodes. 1 or 2 single conductor cables (usually on reels) with proper length for infinite electrode connection. They are necessary only for measurement of pole-dipole and pole-pole arrays. Recommended power source is car battery or AC/DC converter. Recommended software for data interpretation is Res2DInv (resp.Res3DInv).）

Measuring parameters

VES, RP and SP measurement passes in a grid of points (profiles, stations). You are asked to set P-step, S-step and the position of the first measured point before the beginning of the measurement.

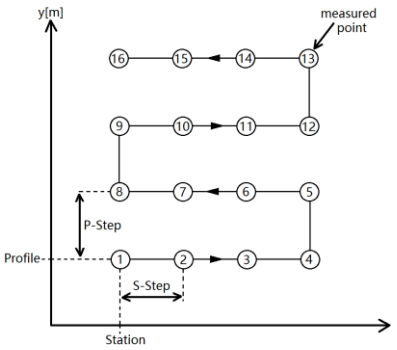

Fig.5 VES, RP and SP positioning

Note: If 10-ch Pole-Dipole array is measured in resistivity profiling (RP) and if measured data are to be interpreted in 2D or 3D model (by means of software Res2DInv resp. Res3DInv) it is necessary to choose S-Step as an integer multiple of coefficient a (a is the distance between potential electrodes) (Fig.5).

Measuring methods

We can choose an electrode array for each method of measurement except self-potential measurement (SP). Various measuring arrays are convenient for optimum sensitivity for different kinds of structures (vertical/horizontal structures, cavities). (Auken E, Nebel L, et al, 2002. Christensen NB, 2002. Danielsen JE, Auken E, et al, 2003. Auken E, Christiansen AV, et al, 2004.)

For infinite electrodes (pole-dipole, dipole-dipole), they are always placed on a fixed position outside the measured profile. Infinite electrodes should be at least 5 times farther apart than the maximum current electrode distance of the measured array. Only in that case can the influence of infinite electrodes be omitted (the error is less than 5%). In case of impossibility to ensure sufficient distance the positions of infinite electrodes can be included in calculation of the geometric factor.

Exact geometric factor – The geometric factor is calculated exactly; positions of infinite electrodes are included.

Approximate geometric factor – Simplified calculation of geometric factor; position of infinite electrodes are not included.

Several preprogrammed electrode arrays can be chosen for resistivity profiling or new electrode configuration can be defined.

Basic arrays are preprogrammed as single-channel ones, i.e. for measurement of them 4 electrodes are needed. Each array is given by its type and parameter a, resp. The result of the measurement of basic array is a curve of apparent resistivity and IP on measured profile (ID), or a map (2D). The more details show in Fig.6.

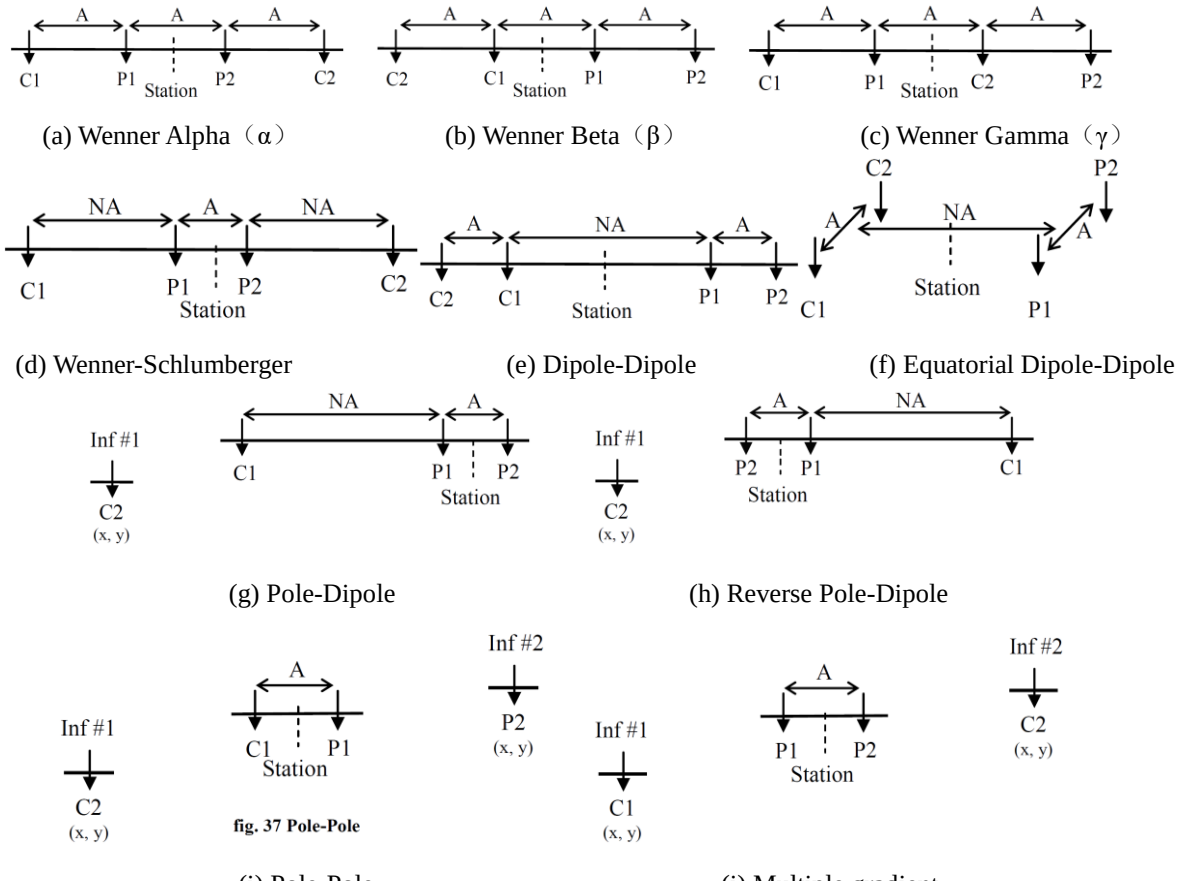

(a) Wenner Alpha（α） (b) Wenner Beta（β） (c) Wenner Gamma（γ）

(d) Wenner-Schlumberger (e) Dipole-Dipole (f) Equatorial Dipole-Dipole

(g) Pole-Dipole (h) Reverse Pole-Dipole

fig. 37 Pole-Pole

(i) Pole-Pole (j) Multiple gradient

Fig.6 Positions of electrodes in different kinds of measuring methods

Besides basic configuration two special arrays can be selected: 10-ch Pole-Dipole, 10-ch General Array. (Advanced Geosciences Inc, 2002. Baker SS, Cull JP, 2004.)

Use of multi-channel system ARES II allows measuring of several depths at once. Values from different depths can also be interpreted in 2D or 3D model, e.g. by means of Res2DInv respectively Res3DInv software. For proper interpretation it is necessary to keep the orientation of the electrodes in the direction of the profile, and to choose the coefficient as an integer multiple of coefficient a.

Beside parameters a, na the parameter Dipoles-count is also defined, which determines the number of channels used for measurement. Channels from R0 to R9 are measuring potential between electrodes from P1-P2 to P10-P11. General array is a universal array, which allows the setting of any electrodes as infinite (called static) or moveable. Infinite (static) electrode has

constant x, y position against the position Profile = 0, Station = 0. Moveable electrode is included in the array moved over profile, its position dx, dy is defined against the point of registration (Profile, Station). Optionally, all or only some channels of the receiver can be activated.

Forward modeling and Inversion simulation

The experiment was carried out in a glass slot in the Civil & Environment Engineering Lab laboratory, which was divided into three stages: (1) glass tank test; (2) dry sand groove test; (3) wet sand tank test. Fig.7-8 show the basic specification of the glass slot and the position of plastic tube.

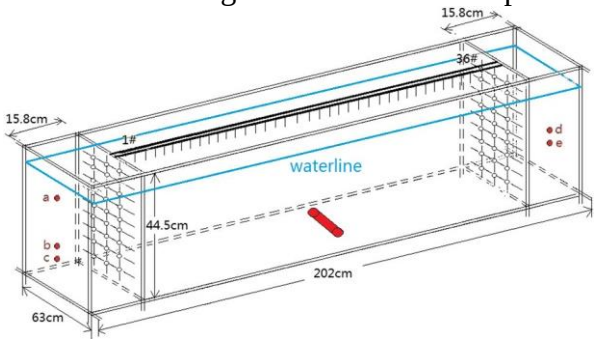

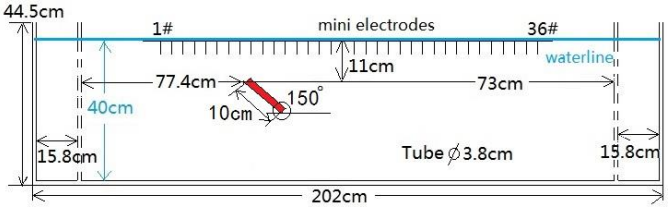

Fig.7 Diagram of glass tank size **Fig.8 Diagram of flume glass tank ERT monitoring electrode arrangement**

This test glass trough material is toughened glass whose waterproof property is good, and the glass wall thickness is 1cm.The specification is: the length of the glass slot (including the wall thickness) is 202cm, the width is 63cm, and the height is 44.5cm. On the side wall of the two sides of the net, the distance from the wall to the wall of the glass slot is 15.8cm, and the mesh side wall has many rules, which are convenient for the experiment of seepage flow and provide the conditions for the experiment of the water flow field in the sand trough. In the back side, there are round hole d, circular hole e, and the vertical height of the circular hole center to the bottom of the glass groove is 8cm and 16.5cm. (The diameter of the round hole is 1.3cm, and the hole of the round hole is blocked with a nut). The glass tank internal and external unit coupling in glass glue bond coupling, need to test whether there is a leakage before the experiment, if not, need to reopen the cementation coupling. Finally, the glass tank is completely airtight sealed.

The glass tank test is used as a pure medium conductor with running water, and the small electrode is a stainless-steel needle. The electrode is arranged on a rectangular thin board with a length of 170.1cm, which is convenient to float in the water surface of the tank. The 36 electrodes are arranged according to the spacing of 4.5cm, and 6.3cm distance is set apart at each end of the board, as shown in figure 13.The small electrodes of the same size are evenly arranged on the small wooden board, and the same depth of the board is inserted into the water surface, which can be considered as the water depth of the small electrode.

The three-dimensional coordinate system is established as shown in figure 12. The length of the tank is the positive direction of the X axis and the width is the positive direction of the Y-axis, and the height is the Z-axis direction. At this point, line 1 electrode number is 36, the electrode spacing is 4.5cm, line the total length of 157.5 1cm, electrode serial number from the front view YZ surface tank to tank back view the YZ plane of 1 ~ # 36, the coordinates in the following table 1.

Table1 List of line electrode coordinate unit

No.	X/cm	Y/cm	Z/cm	Point no.	No.	X/cm	Y/cm	Z/cm	Point no.
1	22.1	31.5	40	A1	19	103.1	31.5	40	B7
2	26.6	31.5	40	A2	34	107.6	31.5	40	B8

3	31.1	31.5	40	A3	35	112.1	31.5	40	B9
4	35.6	31.5	40	A4	36	116.6	31.5	40	B10
5	40.1	31.5	40	A5	37	121.1	31.5	40	B11
6	44.6	31.5	40	A6	38	125.6	31.5	40	B12
7	49.1	31.5	40	A7	39	130.1	31.5	40	B13
8	53.6	31.5	40	A8	40	134.6	31.5	40	B14
9	58.1	31.5	40	A9	41	139.1	31.5	40	B15
10	62.6	31.5	40	A10	42	143.6	31.5	40	B16
11	67.1	31.5	40	A11	43	148.1	31.5	40	B17
12	71.6	31.5	40	A12	44	152.6	31.5	40	B18
13	76.1	31.5	40	B1	45	157.1	31.5	40	B19
14	80.6	31.5	40	B2	46	161.6	31.5	40	B20
15	85.1	31.5	40	B3	47	166.1	31.5	40	B21
16	89.6	31.5	40	B4	48	170.6	31.5	40	B22
17	94.1	31.5	40	B5	49	175.1	31.5	40	B23
18	98.6	31.5	40	B6	50	179.6	31.5	40	B24

(The measurement point A represents 1 channel, and B represents 2 channels)

The small scale crack monitoring physical simulation test is mainly used to monitor the physical response under the condition of uniform medium in water with the monitoring electrode device of the ERT monitoring device. The measurement steps are as follows (Fig.9):

(1) Putting the small diameter 2cm and length 5cm PVC sealed tube into the middle bottom of the glass cistern, which is below the center off the measuring line. The three-dimensional coordinates in the tank are (101cm, 31.5cm, 0cm).

(2) Setting the small diameter 2cm and length 5cm PVC sealed tube into the middle bottom of the glass tank, which is below the center of the measuring line. The three-dimensional coordinates in the tank are (101cm, 31.5cm, 0cm).The small scale fissures are in the middle of the tank as shown in fig.14. The length of the tank is the positive direction of the X axis and the width is the positive direction of the Y-axis, and the height is the direction of the Z-axis.

(3) During the test, the PVC cylinder that simulates small scale cracks will be moved regularly, which will form a contrast.

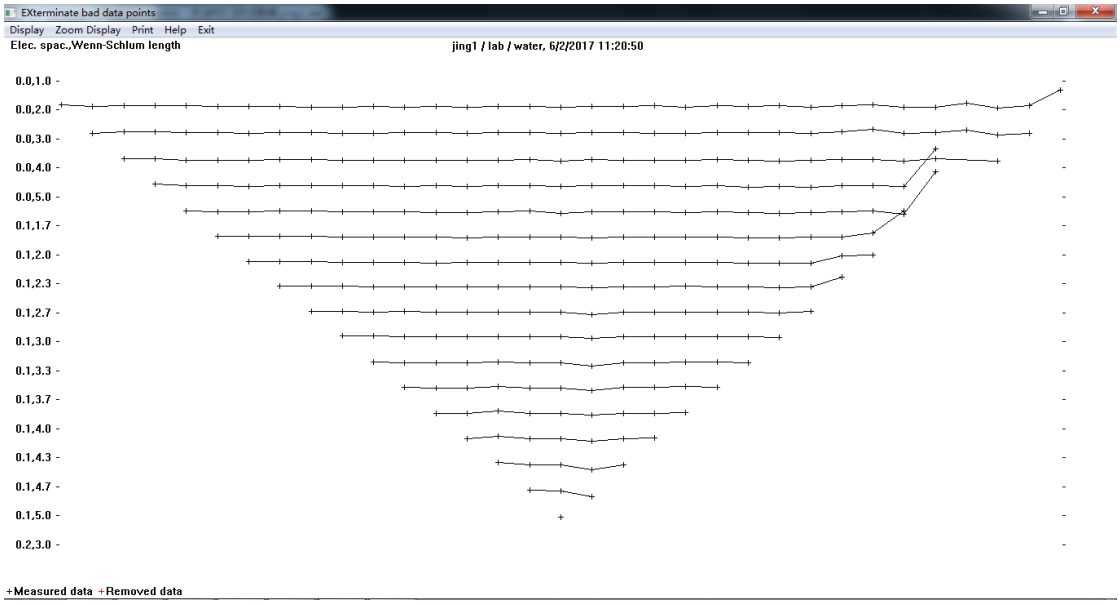

Fig.9 Original data point diagram of the pure water medium in the small scale crack of glass tank

Preliminary analysis of the results showed that the resistivity of the bottom of the water

medium was high and the resistivity of the upper pure water was relatively low. The high resistivity of the bottom may be due to the plastic causes at the bottom of the tank, resulting in the boundary effect. See Fig.10.

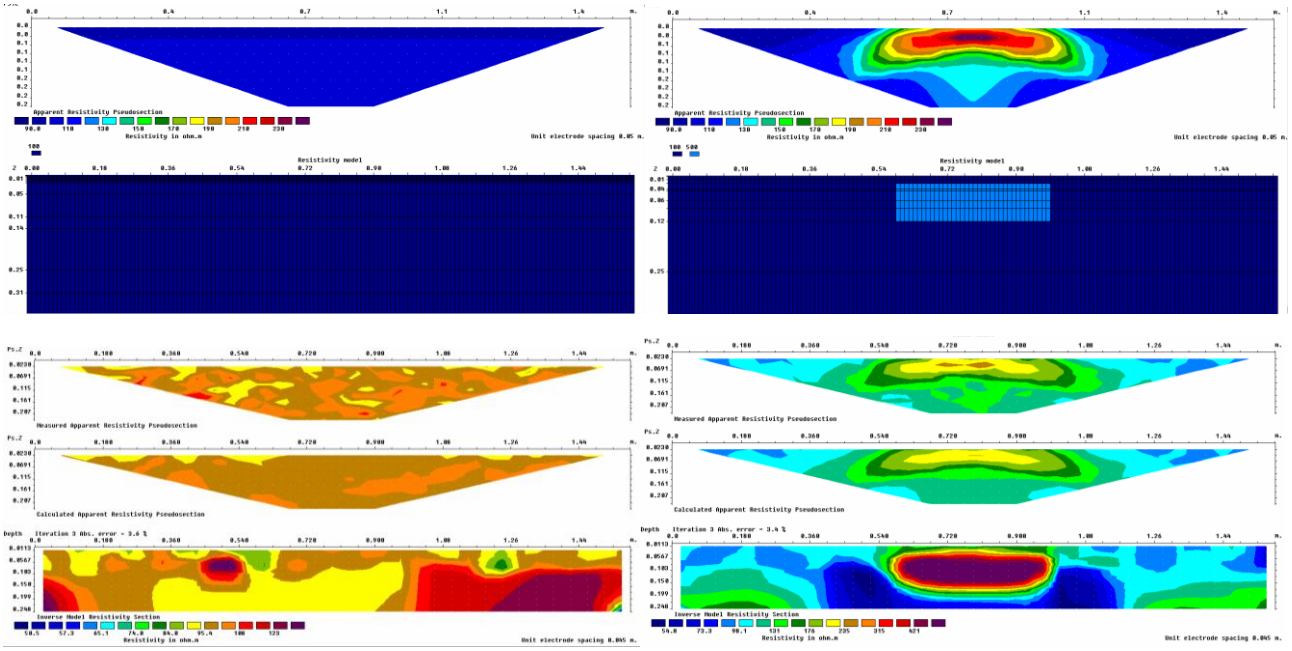

(a) Res2dinv, Res2dmod forward modeling and inversion of pure water

(b) Res2dinv, Res2dmod forward modeling and inversion of PVC tube

Fig.10 Original data point diagram of the pure water medium in the small scale crack of glass tank

Using the Swedish high density software Res2DMOD and Res2DINV, a positive inversion was carried out for the width of 2cm and the length of 10cmPVC tube model. The simulated fracture was in the water conductivity of low resistance medium (such as water).Pure water rho = 100 Ω m. PVC pipe rho = 500Ω.m, tank rho = 2000000 Ω m. Array (Wenner-Schlumber).

Using Res2D INV software for 2D inversion. The Fig. 11 for pure water condition placing a block high resistance body figure, is the blue area as the pure water medium. Water resistivity value is 100Ω.m, abnormal body resistivity value is set to 500Ω.m. Pure sand medium resistivity value is 2500Ω.m and tank resistivity value is 2000000Ω.m.The forward Array is Array (Wenner-alpha).The abnormal body specification is 20cm in length and 3cm in diameter. High resistance body is PVC solid plastic pipe, and low resistance is iron pipe. The detection system is 1.58m in length and the detection electrode is 4.5cm. The detection target position is 10cm depth below the surface of the detection system.

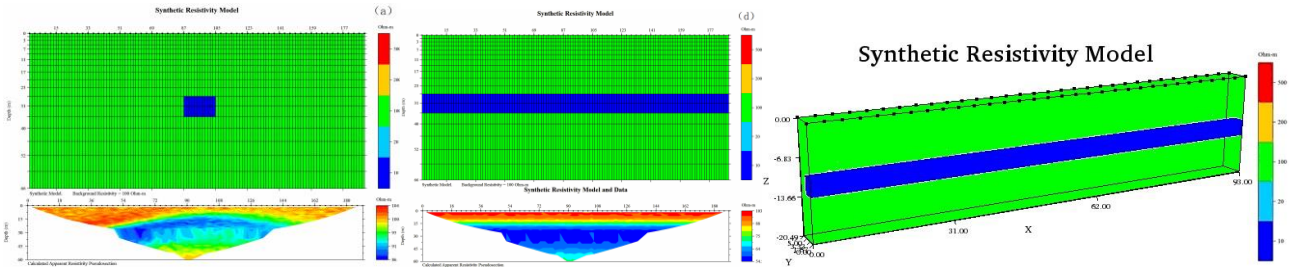

Fig.11 High and low resistivity AGI two-dimensional forward modeling and exploration design abnormal response graph (Wenner - Schlumber)

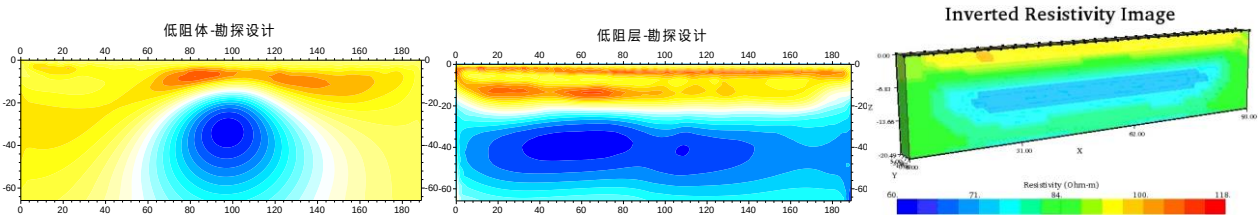

Fig.12 High and low resistivity AGI two-dimensional Inversion simulation and exploration design abnormal response graph (Wenner - Schlumber)

Using Res2D INV software for 2D forward modeling, which Fig.11 for pure water condition placing a block low resistance body figure. The blue area is the pure water medium, water resistivity value is 100Ω.m, abnormal body resistivity value is set to 500Ω.m. The following Fig.12 is a single block of low resistance in the pure water condition. The visual section and resistivity model diagram are shown. The Inversion Array adopts the Array (Wenner-alpha), and the Inversion algorithm adopts Least squares (Least squares).

Experimental tests

In detecting crack fracture in glass tank simulation tests, using GF Instruments company ARES II (Automatic resistivity IP system & instrument). Small stainless-steel needle is used for measuring electrode. The multi-electrode cable adopts 32 measuring channel cable 2, with 64 electrodes in total. The process of experiments see Fig.13.

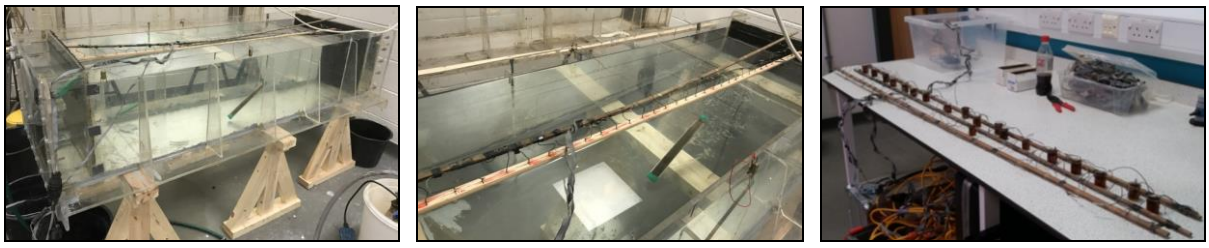

(a) Model experimental tank (b) PVC pipe fracture model (c) Miniature copper electrode

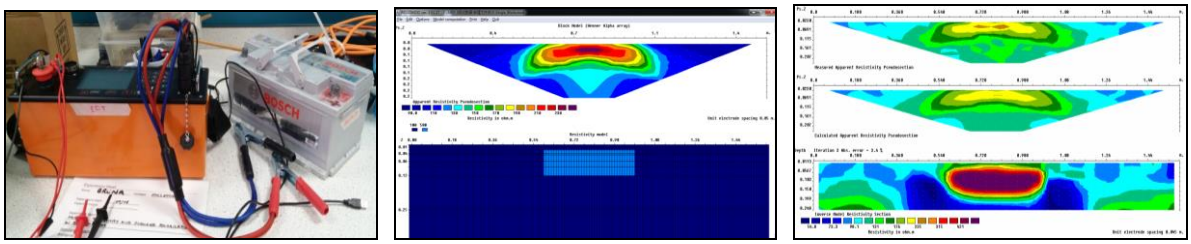

(d)Test instruments and equipment (e) Forward modeling of crack (f) Inversion simulation of crack

Fig.13 Physical model test procedure flow charts of the small scale crack in glass tank

(a) The water tank is organic silicate glass with a size of 202cm*63cm*44.5cm and the water tank is full of pure water. The waterline is 40cm. (b) PVC tube for organic silicide glass material, the size of tube is 1cm by 10cm ⌀, PVC tube stands for crack channel. The position of the top of the PVC tube is 49.5cm in athwart and 11cm below the waterline. The dip angle of the PVC tube is nearly 30 degree. (c) The microprobe electrode sequence is made of copper with a length of 3cm, a single side line and 64 electrodes in it. During the experiments, it is very important to make sure every single electrode is well conducted electric and immersed into the water. (d) GF Instruments company ARES II (Automatic resistivity & IP system), power car batteries. The voltage needed is up to 24 volt. (e) Using high density forward modeling software Res2DMOD, Sweden resistivity of

PVC is 500Ω.m, resistivity of tank is 2000000Ω.m. For more details see Fig.10. (f) Using the Swedish high density software Res2DINV for inversion simulation. For more details see Fig.11 and Fig.12.

CONCLUSION

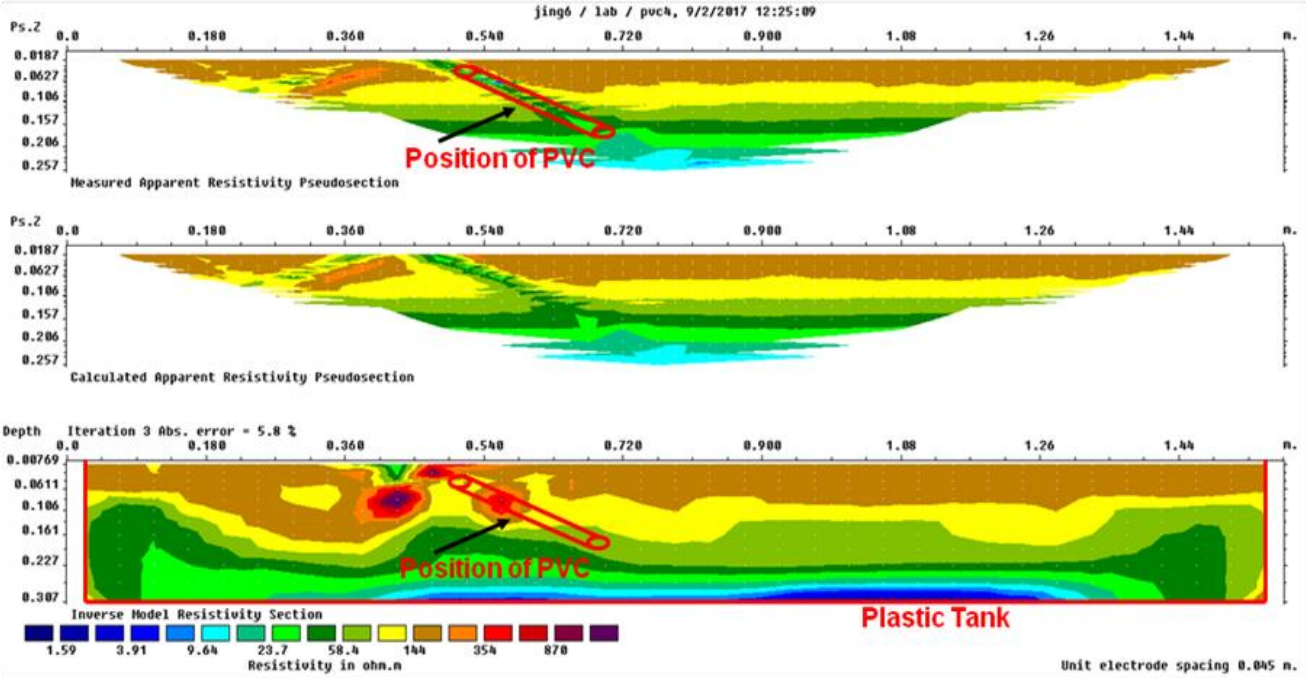

Fig.14 The physical characteristic response of the small scale crack in glass tank

The results of small scale fissure monitoring physical simulation test are shown as shown in the figure 14. As you can see, blue represents low resistivity and red represents high resistivity. There is an obvious low resistivity channel in the middle of the sink. The position of low impedance channel in the figure is consistent with the position of PVC pipe in the tank, and the effect size is good. Meanwhile, because of the boundary effect, the length of low impedance channel is much longer than the real size of the PVC tube. There are several good ideas for future work, if given more time for experiments. Such as using the sand to replace the pure water and mixing the pure water and dry sand, using the iron tube to contrast the effect of the plastic PVC tube. There must be some differences between them, and some relationship between the apparent resistivity measured by ERT and the varieties of conduct electricity Medias. For now, the author is working on the application of ERT in engineering and corresponding affects to rock fracture. He will explain in more detail in next paper, which will be titled “Effect of apparent resistivity of ERT and wave velocity of multichannel transient surface waves in the isotropic rock medium in Gansu province”.

REFERENCE

Advanced Geosciences Inc (2002). Earth Imager, 2D Resistivity and IP Inversion Software.

Baker SS, Cull JP (2004). Streaming potential and groundwater contamination. Exploration Geophysics 35:41-44.

Buselli G, Lu K (2001). Groundwater contamination monitoring with multichannel electrical and electromagnetic methods. J Apply Geophysics 48:11-23.

Maineult A, Barnab é Y, Ackerer P (2004). Electrical response of flow, diffusion, and advection in a laboratory sand box. Vadose Zone J 3:1180-1192.

Nimmer RE, Osiensky JL (2002). Using mise-a-la-masse to delineate the migration of a

conductive tracer in partially saturated basalt. Environmental Geosciences 9:81-87.

Revil A, Naudet V, Nouzaret J and Pessel M (2003). Principles of electrography applied to self-potential sources and hydrogeological applications. Water Resources Res 39: 1114.

Rizzo E, Suski B, Revil A, Straface S, Troisi S (2004). Self-potential signals associated with pumping tests experiments. J Geophysics Res 109:B10203.

Atekwana EA, Werkema DD, Duris JW, Rossbach S, Atekwana EA, Sauck WA, Cassidy DP (2004). In-situ apparent conductivity measurements and microbial population distribution at a hydrocarbon contaminated site. Geophysics 69:56-63.

Berger W, Börner F, Petzold H (2001). Consecutive geoelectric measurements reveal the downward movement of an oxidation zone. Waste Management.21:117-125.

Berthold S, Bentley LR, Hayashi M (2004). Integrated hydrogeological and geophysical study of depression-focused groundwater recharge in the Canadian prairies. Water Resource 40: 1029-1039.

Boerner FD (2001). A novel study of the broad band complex conductivity of various porous rocks. Proc 2001 International Symposium of the SCA, Edinburgh, UK, SCA-2001-38.

Comas X, Slater L (2004). Low frequency electrical properties of peat. Water Ressources Research 40 W12414.

Fechner T, Boerner FD, Richter T, Yaramanci U, Weihnacht B (2004). Lithological interpretation of the spectral dielectric properties of limestone. Near Surface Geophysics: 150-159.

Dresden. Grissemann C, Rammlmair D, Siegwart C, Foullet N (2000). Spectral induced polarization linked to image analyses: A new approach. In: Rammlmair et al. (eds) Applied mineralogy. Balkena, Rotterdam pp 561-564.

Kemna A (2000). Tomographic inversion of complex resistivity. PhD-Thesis. Berichte des Inst. Geophysik der Ruhr-Universität Bochum, Reihe A, 56.

Kemna A, Binley A, Slater L (2004). Crosshole IP imaging for engineering and environmental applications. Geophysics 69: 97-107.

Klitsch N (2003). Ableitung von Gesteinseigenschaften aus Messungen der spektralen induzierten Polarisation a Sedimentgesteinen. PhD-Thesis, Inst Geophysik and Geol Univ Leipzig und Inst Angewandte Geophysik RWTH Aachen.

Lesmes DP, Frye KM (2001). Influence of pore fluid chemistry on the complex conductivity and induced polarization responses of Berea sandstone. Journal of Geophysical Research 106:4079-4090.

Liu S, Yeh T-CJ (2004). An integrativ Approach for monitoring water Movement in the vadose zone. Vadose Zone Journal 3:681-692.

Niederleithinger E, Grissemann C, Rammlmair D (2000). SIP geophysical measurements on slag heaps: A new way to get information about subsurface structures and petrophysical parameters. In: Rammlmair et al. (eds) Applied mineralogy, Balkena, Rotterdam.

Slater LD, Lesmes DP (2002a). Electric-hydraulic relationships observed for unconsolidated sediments. Water ressources research 8:-13.

Slater LD, Lesmes DL (2002b). IP interpretation in environmental investigations. Geophysics 7:7-88.

Titov K, Komarov V, Tarasov A, Levitski A (2002). Theoretical and experimental study of time-domain induced polarization in water-saturated sands. Journal Applied Geophysics 50:417-433.

Titov K, Kemna A, Tarasov A, Vereecken H (2004). Induced polarization of unsaturated sands determined through time domain measurements. Vadose Zone Journal 3:1160-1168.

Ulrich C, Slater LD (2004). Induced Polarization on unsaturated, unconsolidated sands. Geophysics 68:762-771.

Weihnacht B, Boerner F (2005). Ermittlung geohydraulischer Parameter aus kombinierten geophysikalischen Messungen im Technikumsmaßstab. Proc. 65. JT der DGG, Graz, p. 39.

Ahl A (2003). Automatic 1D inversion of multifrequency airborne electromagnetic data with artificial neural networks: discussion and case study. Geophysical Prospecting 51:89-97.

Bosch FP, Gurk M (2000). Comparison of RF-EM, RMT and SP measurements on a karstic terrain in the Jura Mountains (Switzerland). Proceed of the Seminar Electromagnetische Tiefenforschung Deutsche Geophysikalische Gesellschaft: 51-59.

Auken E, Jørgensen F, Sørensen KI (2003). Large-scale TEM investigation for ground-water. Exploration Geophysics 33:188-194.

Auken E, Nebel L, Sørensen KI, Breiner M, Pellerin L, Christensen NB (2002). EMMA - A Geophysical Training and Education Tool for Electromagnetic Modeling and Analysis. Journal of Environmental & Engineering Geophysics 7:57-68.

Christensen NB (2002). A generic 1-D imaging method for transient electromagnetic data. Geophysics 67:438-447.

Danielsen JE, Auken E, Jørgensen F, Søndergaard VH, Sørensen KI (2003). The application of the transient electromagnetic method in hydrogeophysical surveys. Journal of Applied Geophysics 53:181-198. 114:433-442. soundings. Geoexploration 24:131-146.

Auken E, Christiansen AV, Jacobsen L, Sørensen KI (2004). Laterally Constrained 1D-Inversion of 3D TEM Data. 10th meeting EEGS-NS, Utrecht, The Netherlands, EEGS-NS. Extended Abstracts Book.

ACKNOWLEDGEMENT

The authors wish to acknowledge the support of the European Commission via the Marie Curie IRSES project GREAT ‘Geotechnical and geological Responses to climate change: Exchanging Approaches and Technologies on a world-wide scale’ (FP7-PEOPLE-2013-IRSES-612665). This paper is for the special session of "Geophysics for Urban Underground Space Development". The author would like to thank Prof. Liu Lan-bo for offering this so precious opportunity to publish their work on Symposium on the Application of Geophysics to Engineering and Environmental Problems (SAGEEP). It is particularly grateful to Prof. Li Xiao-zhao for supporting author to exchange his idea of this paper with Prof. Alessandro Tarantino. And appreciating Prof. Alessandro Tarantino for helping with these work. The author will keep working in the field of development of refined geophysics application on subsurface structures and petrophysical parameters. The next work will present how to use geophysics technical methods in the rock engineering.